JOURNAL OF MATERIALS SCIENCE 31 (1996) 5773–5779

Combustion synthesis and properties of mullite–zirconia composites

R. GOPI CHANDRAN, K. C. PATIL*
Department of Inorganic and Physical Chemistry, Indian Institute of Science, Bangalore-560 012, India
G. T. CHANDRAPPA
Department of Chemistry, M.S. Ramaiah Institute of Technology, Bangalore-560 054, India

Mullite–zirconia composite powders were prepared by the combustion of an aqueous heterogeneous redox mixture consisting of $Al(NO_3)_3$, $Zr(NO_3)_4/ZrO(NO_3)_2$, silica fume and urea/diformyl hydrazine at 500 °C. X-ray diffraction data showed that a large amount of tetragonal zirconia existed in the composite powders in spite of high temperature calcination. Milled composite powders showed enhanced densification compared to the unmilled powders and the microstructure of the sintered (1600 °C) compacts showed the presence of spherical zirconia grains in intergranular positions along with elongated mullite grains.

1. Introduction

Ceramic matrix composites can offer better performance compared to single phase ceramics. Thus, zirconia inclusions are known to impart desirable mechanical properties such as high toughness and strength when present in composite ceramics [1–3]. Mullite ceramics have medium strength and fracture toughness at room temperature, but have notable strength and low creep rate at high temperatures. Improvements in mechanical properties could be achieved by zirconia inclusions (by toughening mechanisms, stress induced transformation or microcracking). Moreover, ZrO_2 is known to clean the grain boundaries and limit grain growth. The potential for improved performance is, however, offset by increased difficulties in processing. It is rather difficult to prepare composites containing an uniform dispersion of fine particle zirconia in the mullite phase by ceramic processing techniques. Some of the techniques used to prepare mullite–zirconia composites includes reaction sintering of alumina and zircon powders [4–8], sol–gel [9–12], co-precipitation [13], etc. Sacks *et al.* [14] obtained high density compacts using amorphous silica and zirconia-coated corundum particles. Yuan *et al.* [15] prepared mullite powders by the sol–gel route and then blended it with very fine ($\approx 0.2\ \mu m$) zirconia powders. Zirconia dispersed mullite ceramics were also prepared by sintering mixtures of ZrO_2 and some crystalline/non-crystalline mullite powders [16].

A low-temperature initiated, self-propagating, gas-producing combustion process has been used successfully for the preparation of mullite [17, 18], chromites [19], cuprates [20], cordierite [21], ZrO_2 [18, 22], and Al_2O_3–ZrO_2 composites [23, 24]. In this paper, we report the synthesis and properties of mullite–zirconia composites by the combustion method.

2. Experimental procedure

2.1. Combustion synthesis of mullite–zirconia composites

The stoichiometry of the redox mixture used for the synthesis of mullite–zirconia composites was calculated by a procedure similar to that for mullite [17, 18]. The stoichiometry of the redox mixtures used for combustion were calculated using the total oxidizing and reducing valencies of the components which serve as numerical coefficients for the stoichiometric balance so that the equivalence ratio (ϕ_e) is unity and the energy released by combustion is maximized. According to this concept the valence of C = + 4, H = + 1, divalent metal ions = + 2, trivalent metal ions = + 3 and so on, and O = − 2. The valence of nitrogen is considered to be zero. Based on these considerations aluminium nitrate will have an oxidizing valence of − 15 diformyl hydrazine ($C_2H_4N_2O_2$, DFH) will have a reducing valence of + 8.

Mullite–zirconia composites have been prepared by the combustion of aluminium nitrate, zirconium nitrate/zirconyl nitrate, silica fume (surface area $\approx 200\ m^2\ g^{-1}$) and urea/DFH at 500 °C. A redox mixture containing 0.05 moles of aluminium nitrate was used for each reaction. 3 mol % of $Mg(NO_3)_2 \cdot 6H_2O$, corresponding to the amount of zirconium, was added to the redox mixture used for combustion. When inserted into a furnace preheated to 500 °C, the redox

*Author for correspondence.

0022–2461

mixture initially boils, froths and ignites to burn with a flame to give voluminous products.

The composites prepared using zirconium nitrate ($Zr(NO_3)_4 \cdot 5H_2O$) and zirconyl nitrate ($ZrO(NO_3)_2 \cdot 2H_2O$) are referred to as MZ and MZO, respectively. A final letter U or D denotes the use of the urea or the silica fume process, with the wt % of zirconia being given in the numeric suffix. For example MZOU20 refers to mullite containing 20 wt % of zirconia prepared by the combustion of aluminium nitrate, zirconyl nitrate, silica fume and "urea". Similarly MZD20 refers to mullite containing 20 wt % of zirconia prepared by the combustion of aluminium nitrate, zirconium nitrate, silica fume and "DFH".

2.2. Physical measurements

The formation of mullite–zirconia composites has been confirmed by powder X-ray diffraction (XRD), recorded using a Philips PW 1050/70 X-ray diffractometer using CuK_α radiation and a Ni filter. Particle size analysis was done on a Seishin Micron Photosizer model SKC 2000 which operates on the light scattering principle employing sedimentation. The temperature of the incandescent flame which appears during the combustion process was measured using an optical pyrometer model-120 made by Toshniwal Company, India. For sintering studies, mullite–zirconia powders were ground for 3 h using an electric agate pestle and mortar and were uniaxially compacted at 50 MPa. Bulk densities of the sintered compacts were measured by Archimedes' principle using distilled water. Microstructures of the sintered samples were observed using a S-360 Cambridge scanning electron microscope (SEM) and chemical composition was determined by an energy dispersive X-ray (EDX) detector attached to the SEM.

The fraction of tetragonal zirconia (t-ZrO_2) (F_t) present in the composite powder calcined at 1600 °C for 2 h, was estimated using the equation [25]

$$F_t = \frac{I_t(1\,1\,1)}{I_t(1\,1\,1) + I_m(1\,1\,1) + I_m(1\,1\,\bar{1})}$$

where $I_t(1\,1\,1)$, $I_m(1\,1\,1)$, and $I_m(1\,1\,\bar{1})$ refer to the intensity of (1 1 1) reflection of tetragonal, monoclinic, and (1 1 $\bar{1}$) reflection of monoclinic zirconia, respectively.

3. Results and discussion

Redox mixtures containing zirconyl nitrate, aluminium nitrate and urea are known [24] to yield uniformly dispersed t-ZrO_2/Al_2O_3 powders on combustion. The mixture containing silica fume when rapidly heated at 500 °C behaved similarly to yield foamy products. The powder XRD patterns of as-formed MZU20, MZOU20, MZOD30, and MZOU30 are given in Fig. 1. The products derived from the urea process was crystalline while it was amorphous in the case of the DFH process (containing 20 wt % ZrO_2). However, the as-formed mullite–zirconia powders (MZOD30) showed the presence of t-ZrO_2. The crystallite size of t-ZrO_2 calculated from X-ray line broadening in the XRD pattern in the as-prepared composite powder was 20–30 nm. XRD patterns of composites (20 and 30 wt %) heated at 1400 °C for 2 h and cooled are shown in Fig. 2. The XRD pattern of the composites shows the presence of zircon besides mullite and t-ZrO_2. A similar behaviour has been reported in the case of co-precipitated composite powders [13]. Therefore, it is evident that the aluminosilicate species crystallize as mullite and zircon between 1300 and 1400 °C in the presence of zirconia.

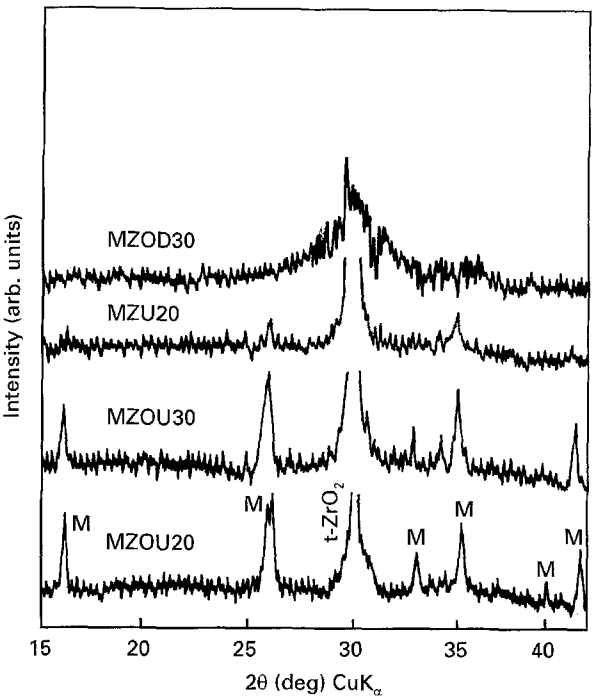

Figure 1 Powder XRD pattern of as-formed mullite–zirconia composites.

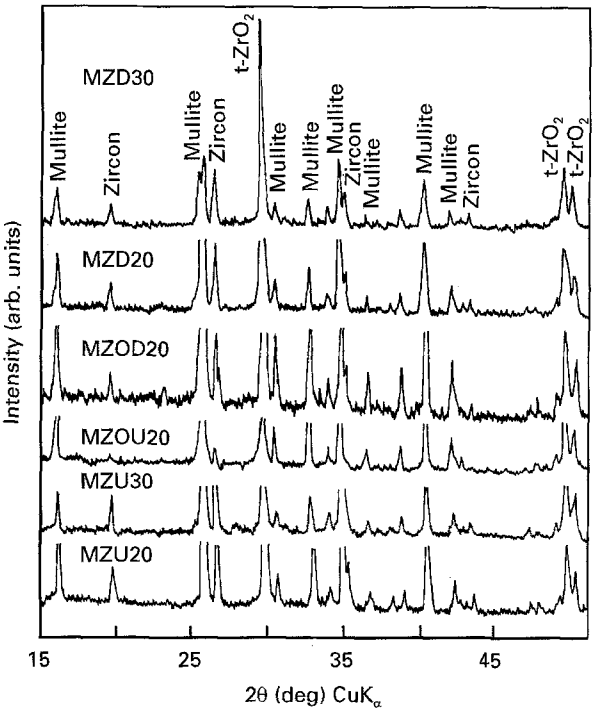

Figure 2 Powder XRD pattern of mullite–zirconia composites calcined at 1400 °C for 2 h.

TABLE I Temperature-product phase evolution and % t-ZrO_2 of the composite powder calcined at 1600 °C for 2 h

Sample	Temperature (°C)				% t-ZrO_2 (1600 °C, 2 h)
	As-formed	1200	1400	1600	
Urea process					
MZU20	t, M	t, M	t, M, Z	t, M, m	59
MZU30	t, M	t, M	t, M, Z	t, M, m	63
MZOU20	t, M	t, M	t, M, Z	t, M, m	67
MZOU30	t, M	t, M	t, M, Z	t, M, m	66
DFH process					
MZD20	a	t	t, M, Z	t, M, m	64
MZD30	t	t	t, M, Z	t, M, m	47
MZOD20	a	t	t, M, Z	t, M, m	60
MZOD30	t	t	t, M, Z	t, M, m	53

t = t-ZrO_2, m = m-ZrO_2, M = Mullite, Z = Zircon ($ZrSiO_4$), a = amorphous.

TABLE II Relative densities of mullite–zirconia compacts sintered at 1600 °C for 2 h

Specimen	Average size (μm) (from sedimentation)	Theoretical density (%)
Urea Process		
MZO10	10.2	56.3
MZO20	12.9	58.8
MZO30	13.8	62.1
MZO20-milled	8.3	73
MZ20	6.8	60.1
MZ30	10.1	64.4
DFH process		
MZO10	4.3	60
MZO20	4.5	71.7
MZO30	2.7	74.6
MZO20-milled	2.8	86
MZ20	4.2	70.1
MZ30	3.5	78.2
Pure mullite		
Urea Process-unmilled	8	51
Urea Process-milled	4	61
DFH Process	3.88	56

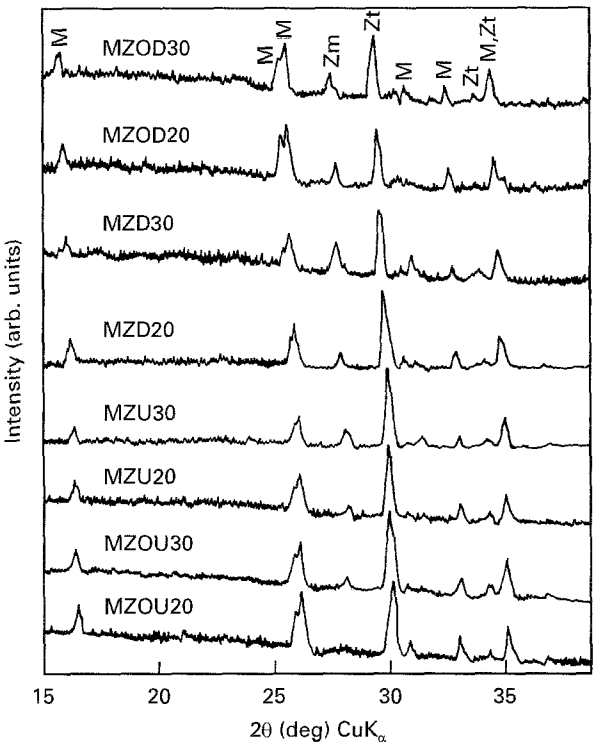

Figure 3 Powder XRD pattern of heat treated (1600 °C for 2 h) mullite–zirconia composites (M = Mullite, Zm = m-ZrO_2 and Zt = t-ZrO_2).

However, specimens calcined above 1500 °C showed XRD patterns of mullite and zirconia phases only.

The XRD patterns of composite powders calcined at 1600 °C for 2 h are given in Fig. 3. The percentage of t-ZrO_2 in composites (20 and 30 wt %) varies from 47–67%. However the percentage of tetragonal zirconia was greater in the sintered body compared to the calcined powder. For example, 83 and 76% of zirconia was retained in tetragonal form in the case of MZOU30 and MZOD30, respectively, in the compact, while it was only 65.8 and 53.1% in the calcined powder. The stabilization of tetragonal zirconia in the composite powders is successfully accomplished by the uniform distribution of fine zirconia particles. In the DFH process *in situ* crystallization of tetragonal zirconia was possible during heating due to the fine size of zirconia and also because of the constraint force of the rigid mullite matrix. The evolution of crystalline phases with temperature were followed and approximate estimates of the quantities of the product were made from the intensities of the appropriate prominent peaks in the diffraction pattern. The different phases formed on calcination and % t-ZrO_2 present in the composites (calcined at 1600 °C for 2 h) are listed in Table I. Zirconia crystallites were essentially tetragonal up to 1400 °C and appreciable amount of monoclinic zirconia (m-ZrO_2) showed up only at 1600 °C (Table II, Fig. 3).

3.1. Sintering and microstructure

The average particle size and the bulk density of the composites prepared by urea and DFH processes are listed in Table II. Typical particle size distribution of

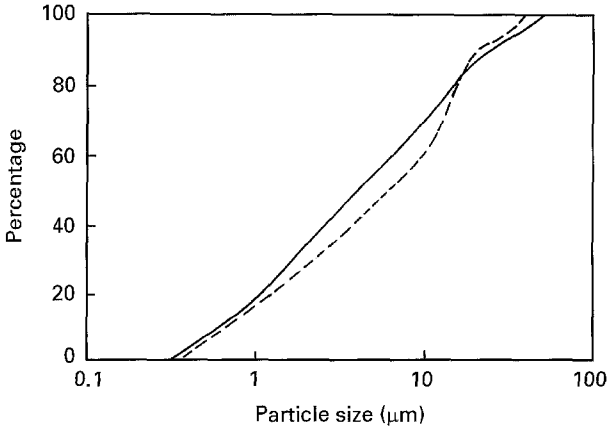

Figure 4 Particle size distribution of as-formed MZU20 and MZD20. Key:— MZD20 (average 4.2 μm); ---- MZU20 (average 6.8 μm).

as-formed MZU20 and MZD20 are shown in Fig. 4. It could be seen that the average size of MZD20 (4.2 μm) is slightly lower than MZU20 (6.8 μm). This could be attributed to the lower flame temperature (1050–1100 °C) of the DFH process in comparison with the urea route (1200–1300 °C).

The bulk density of mullite with 20 wt % of zirconia sintered at 1600 °C for 2 h was 58–72% of theoretical for both urea and DFH processes and about 62–78% with 30 wt% of zirconia while pure mullite was 51% dense. Milling of the powders (Al_2O_3 balls, 4 h) improved the density appreciably. The microstructure of milled and unmilled MZOD20 green compact are shown in Fig. 5. It could be seen that the agglomerates are broken by milling and a reduction in particle size is observed. However, the milling time was not long enough to break all the agglomerates. Typical particle size distribution of MZOD20 milled and unmilled powders are shown in Fig. 6 for comparison. It could be seen that milling reduces the percentage of agglomerates $\geq$ 10 μm. The bulk density of milled MZOD20 at 1600 °C was 86% of theoretical while unmilled powder was only 72%. The relative densities of mullite and mullite–zirconia compacts sintered at 1600 °C are listed in Table II. The bulk density of the composites prepared by the DFH process was greater than that of those by the urea process, probably due to the lower particle size. Incorporation of ZrO_2 (> 20 wt %) resulted in marginal improvement of the density. The observed low density could be attributed to the lower green density of the compact (45%). The finer particle size of zirconia (< 30 nm) results in large agglomerates and low green density. The presence of crystalline mullite in the as-formed powders (urea process) is considered to hinder densification and early sintering of the large agglomerates suppressed further densification and resulted in low density of the sintered compacts. Milling of the powders helped to break the large agglomerates and resulted in improved density compared to the unmilled powder (Table II). It is interesting to note that the density of pure mullite was not enhanced by milling (Table II). However, the addition of zirconia favourably influences the sintering kinetics of mullite (Table II). Similar effect has been observed by a number of workers [5, 12, 13, 15, 16].

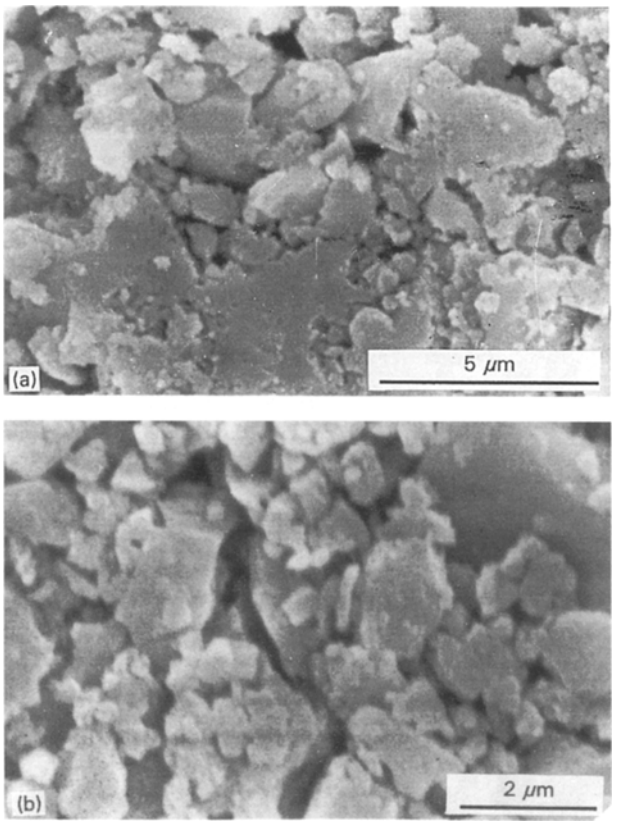

Figure 5 Microstructure of MZOD20 green compact (a) milled and (b) unmilled sample.

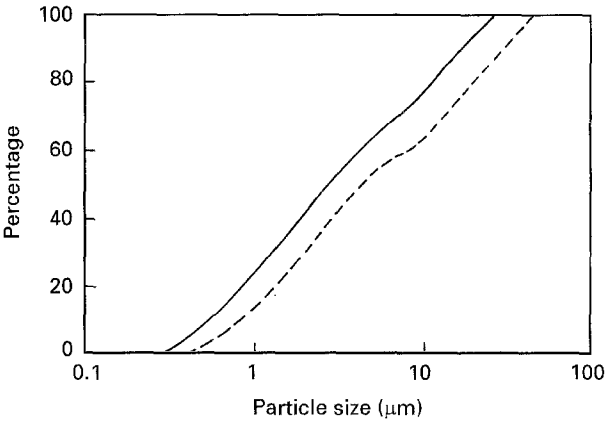

Figure 6 Particle size distribution of MZOD20 milled and unmilled powder. Key:---- MZOD20 unmilled (4.5 μm); — MZOD20 milled (2.8 μm).

Fig. 7 shows the microstructure of mullite–zirconia (20–50 wt %) prepared by the DFH process and sintered at 1600 °C. The EDX (Fig. 7) of the brighter region corresponds to zirconia while darker regions to mullite. Also, the zirconia particles are seen in the intergranular positions with spherical morphology while mullite grains were elongated. This may be due to the formation of SiO_2-rich mullite [16] at elevated temperatures, even though the Al_2O_3: SiO_2 ratio of the composite corresponds to stoichiometric mullite. No other phases except mullite and zirconia were identified by XRD for the composite powders calcined at 1600 °C. It is interesting to note that the zirconia grain size was less than 2 μm. The microstructure of sintered mullite–zirconia composite (20–50 wt %)

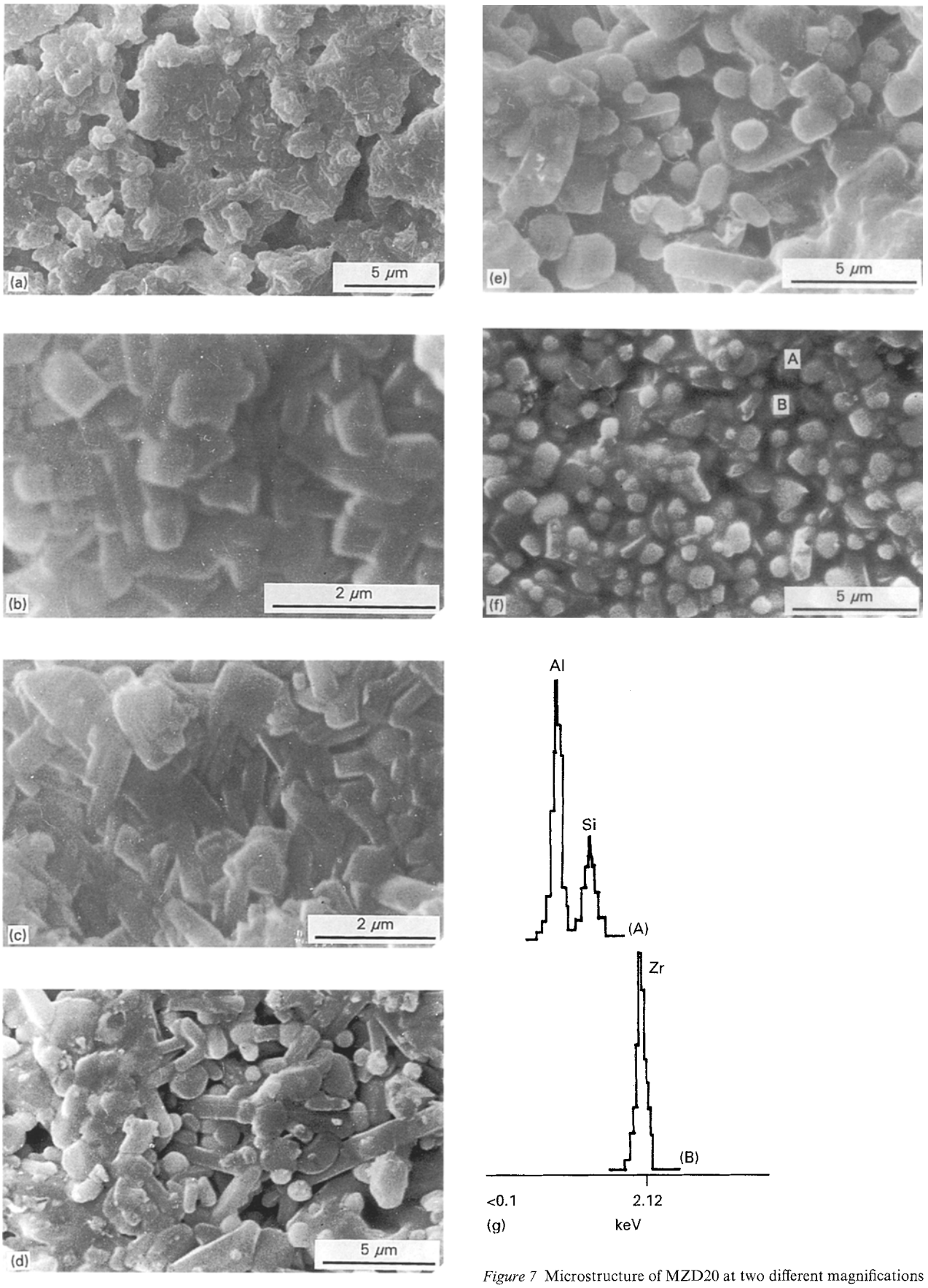

Figure 7 Microstructure of MZD20 at two different magnifications (a) and (b), MZOD20-unmilled (c), MZOD20-milled (d), MZD30 (e), MZOD50 (f) sintered at 1600 °C and (g) EDX of the grains marked A and B in (f).

prepared by the urea process are shown in Fig. 8. The microstructure of MZOU40 (milled, Fig. 8d) sintered at 1600 °C for 2 h (81% dense) shows rounded zirconia with a size of less than 3 μm. However for MZOU50 (unmilled, 71% dense, Fig. 8e) the zirconia grains were no longer rounded. The EDXS of the brighter irregular grain correspond to zirconia while dark elongated grains correspond to mullite. The composition near the mullite–zirconia grain boundary corresponds to zirconia rich aluminosilicate. The XRD of MZOU50

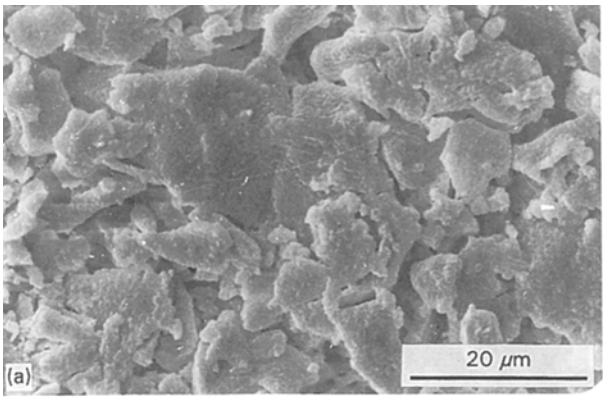

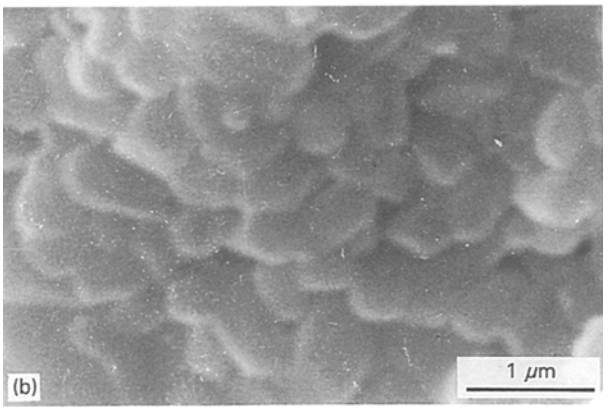

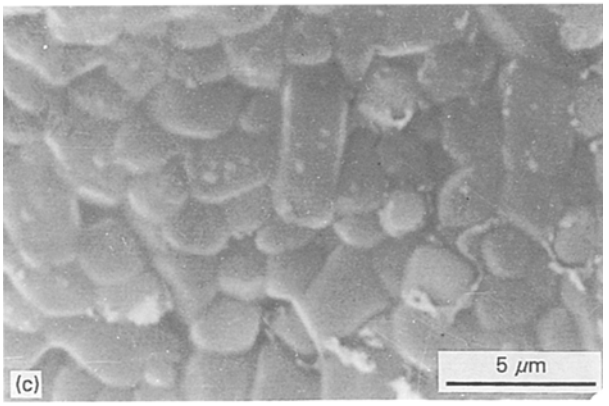

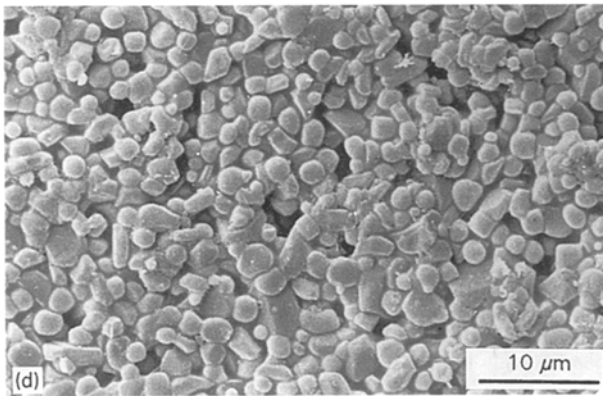

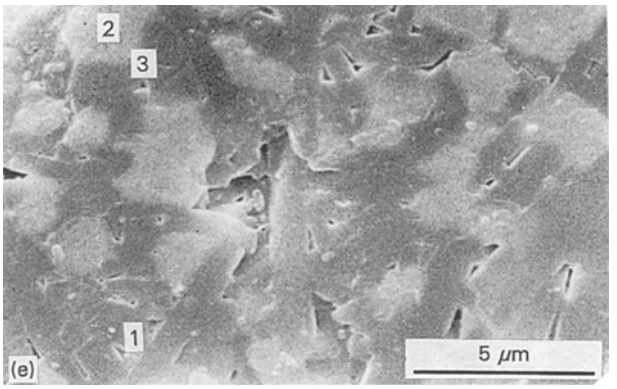

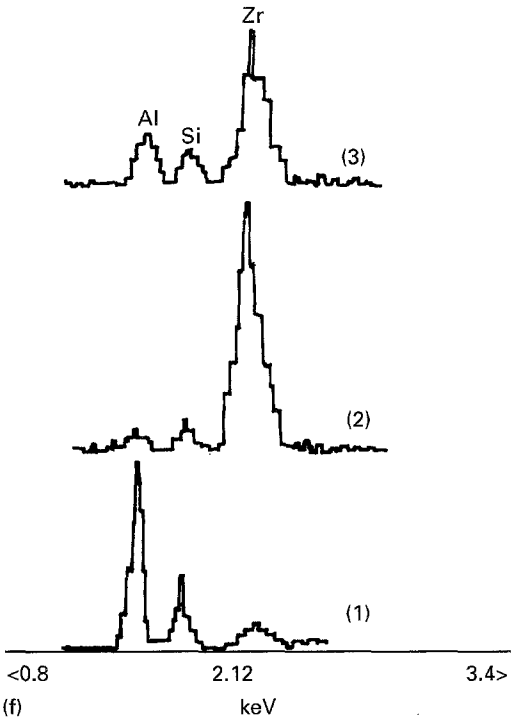

Figure 8 Microstructure of MZU20 at two different magnifications (a) and (b), MZU30 (c), MZOU40-milled (d), MZOU50 (e) sintered at 1600 °C for 2 h and (f) EDX of the grains marked 1, 2 and 3 in micrograph (e).

sintered at 1600 °C shows 65% of monoclinic zirconia indicating that the tetragonal content in the composite decreased with increase in zirconia content. This may be a consequence of enhanced growth of zirconia crystallites to sizes larger than the critical size required for the retention of the tetragonal form on cooling.

4. Conclusions

Fine mullite–zirconia composite powders were prepared by the combustion method using urea and diformyl hydrazine fuels. A large amount of tetragonal zirconia existed in the composite powders after high temperature calcination because of the small particle size of zirconia and the constraint forces of the mullite matrix. Sintered mullite–zirconia composite were porous and greater sintered density was possible by the milling of the starting powders. Total densification of the compacts was not possible because of the low green density and agglomeration of the particles. The microstructure of the sintered mullite–zirconia composite show the presence of spherical intergranular zirconia grains.

Acknowledgements

One of the authors (RGC) is grateful to the Council of Scientific and Industrial Research (CSIR), New Delhi, India for the award of a Senior Research fellowship.

References

1. N. CLAUSSEN and M. RUHLE, in "Advances in Ceramics", Vol. 3, "Science and Technology of Zirconia", Edited by A.H. Heuer and L.W. Hobbs (American Ceramic Society, Columbus, OH, 1981) p. 137.
2. K. T. FABER, in "Advances in Ceramics", Vol. 12, "Science and Technology of Zirconia-II", edited by, N. Claussen, M. Ruhle and A.H. Heuer (American Ceramic Society, Columbus, OH 1984) p. 293.
3. A. H. HEUER, *J. Amer. Ceram. Soc.*, **70**, (1987) 689.
4. N. CLAUSSEN and J. JAHN, *Ibid.* **63** (1980) 228.
5. J. S. MOYA and M. I. OSENDI, *J. Mater. Sci.* **19** (1984) 2909.
6. E. DIRUPO, T. E. CARRUTHERS, and R. J. BROOK, *Ibid.* **71** (1985) 114.
7. P. BOCH and J. P. GIRY, *Mater. Sci. Eng.* **71** (1985) 39.
8. M. F. MELO and M. O. FIGUEIREDO, *Ibid.* **A109** (1989) 61.
9. V. S. NAGARAJAN and K. J. RAO, *J. Solid State Chem.* **88** (1990) 419.
10. Ph. COLOMBAN and L. MAZEROLLES, *J. Mater. Sci.* **26** (1991) 3503.
11. M. NOGAMI and K. NAGASAKA, *Ibid.* **26** (1991) 3665.
12. H. SUZUKI and H. SAITO, *Ibid.* **25**, (1990) 2253.
13. S. RAJENDRAN and H. J. ROSSELL, *Ibid.* **26** (1991) 5815.
14. M. D. SACKS, N. BOZHURT and G. W. SCHERER, *J. Amer. Ceram. Soc.* **74** (1991) 2428.
15. Q. M. YUAN, J. O. TAN and Z. G. JIN, *Ibid.* **69**, (1986) 265.
16. S. PROCHAZKA, J. S. WALLACE and N. CLAUSSEN, *Ibid.* **66** (1983) C-125.
17. R. GOPI CHANDRAN and K. C. PATIL, *Mater. Lett.* **10** (1990) 291.
18. R. GOPI CHANDRAN, G. T. CHANDRAPPA and K. C. PATIL, *Int. J. Self-Prop. High-Temp. Synth.* **3** (1994) 131.
19. R. GOPI CHANDRAN and K. C. PATIL, *Mater. Lett.* **12** (1992) 437.
20. *Idem, Mater. Res. Bull.* **27** (1992) 147.
21. *Idem, Brit. Ceram. Trans.* **92** (1993) 239.
22. N. A. DHAS and K. C. PATIL, *Int. J. Self-Prop. High-Temp. Synth.* **1** (1992) 576.
23. J. J. KINGSLEY and K. C. PATIL, *Ceram. Trans.* **12** (1990) 217.
24. N. A. DHAS and K. C. PATIL, *Ceram. Int.* **20** (1994) 57.
25. R. C. GARVIE and P. S. NICHOLSON, *J. Amer Ceram. Soc.* **55** (1972) 303.

Received 19 October 1994
and accepted 13 February 1996